

PCCP

Accepted Manuscript



This is an *Accepted Manuscript*, which has been through the Royal Society of Chemistry peer review process and has been accepted for publication.

Accepted Manuscripts are published online shortly after acceptance, before technical editing, formatting and proof reading. Using this free service, authors can make their results available to the community, in citable form, before we publish the edited article. We will replace this *Accepted Manuscript* with the edited and formatted *Advance Article* as soon as it is available.

You can find more information about *Accepted Manuscripts* in the [Information for Authors](#).

Please note that technical editing may introduce minor changes to the text and/or graphics, which may alter content. The journal's standard [Terms & Conditions](#) and the [Ethical guidelines](#) still apply. In no event shall the Royal Society of Chemistry be held responsible for any errors or omissions in this *Accepted Manuscript* or any consequences arising from the use of any information it contains.

The PPAR γ helix 12 exhibits an antagonist conformation

Filip Fratev

Institute of Biophysics and Biomedical Engineering, Bulgarian Academy of Sciences,
Acad. G. Bonchev Str., Block 105, 1113 Sofia, Bulgaria

*Corresponding author e-mail: fratev@biomed.bas.bg

Keywords: Peroxisome proliferator-activated receptor gamma (PPAR γ) · helix 12 (H12) · Accelerated Molecular Dynamics (aMD) · Metadynamics · Nuclear receptors (NR)

Abstract

Although the peroxisome proliferator-activated receptor γ (PPAR γ) is one of the most studied nuclear receptors (NR), it is still unknown whether its activation helix (helix 12, H12) could exhibit antagonist conformation as previously demonstrated for most of the NRs. The high H12 flexibility in the apo PPAR γ and the lack of appropriate antagonist ligands complicate the structural and dynamics description by most of the experimental techniques.

Based on intensive ($\approx 12\mu\text{s}$) accelerated molecular dynamics (aMD) simulations together with metadynamics and conventional MD runs, we reveal that H12 could exist in an antagonist conformation. This H12 state and the well known agonist configuration have virtually identical free energy. Notably, significant deviations in the H12 conformations are detected in a homodimer. In chain A the activation helix is stabilized only in a full agonist conformation whereas in chain B, due to the agonist to antagonist states exchanges, H12 is oriented toward helix 4. In summary, the results provide an explanation of the observed asymmetry in most of the PPAR γ homodimer crystal structures. They also suggest selection guidance for protein moieties and structure candidates that would best serve as potential ligand binding sites to achieve stable antagonist form of the receptor.

1. Introduction

PPAR γ is one of the most studied nuclear receptors (NR), but the structural and dynamical properties of its activation helix (H12) in the apo receptor form are still limited. The data

collected by several experimental techniques, including hydrogen deuterium exchange (HDX) mass spectrometry, NMR and fluorescence anisotropy, reveal that H12 and the neighboring structural protein domains, the last portion of helix 11 (H11) and the loop between H11 and H12, are highly flexible. They are however, stabilized solely in response to ligand binding [1–3]. Moreover, the dynamics of the receptor periodically alters its conformational state [3]. This hinders the structural and dynamics H12 properties in the apo receptor by most of the experimental techniques. *In silico* conventional molecular dynamics (cMD) simulations indicate that H12 is located close to the ligand binding domain (LBD) with an ensemble of conformations near the full PPAR γ agonist state [4-5].

Over 130 X-ray PPAR γ holo structures with both partial and full agonist ligands have been solved up to date and they all captured the activation helix in only one, full agonist, state in which the receptor can bind various co-activators. However, in most of the other NRs well defined H12 conformation, named as an antagonist conformation, is also present. In this state H12 undergoes dramatic change in the orientation. From an almost perpendicular position to the helix 3 (H3), as seen in the agonist state, H12 orients parallel to the same helix, allowing co-repressors instead of co-activators binding. Such a conformation has been observed in a PPAR α subtype but never in PPAR γ [6]. This is an interesting difference, which is presumably due to the fact that the first classes of PPAR γ non-covalent antagonist ligands have recently been discovered [7] and their binding mode and H12 dynamics have been described only by cMDs simulations [5]. These simulations suggests for H12 repositioning in response to antagonist binding that is much less pronounced in PPAR γ when compared to the other known NRs. The ligands reshape the co-activators binding pocket rather than establish a typical antagonist activation helix position. However, the existing non-covalent antagonists stabilize the activation helix in new states [5, 8].

One more debate has recently arisen regarding the H12 form in PPAR γ derived from X-ray structures. While in chain A the activation helix is always in a full agonist conformation, independently of the ligand type bound in LBD (partial or full agonist), in chain B its conformation is significantly different (detached from LBD and inclined) in most of the X-ray structures. Notably, both chain A and B H12 are in a full agonist position when bound to a strong agonist, such as Rosiglitazone. Hence, it has been suggested that the distortion in chain B is related to the ligand phenotype (partial agonism) [9-11] and is not just a crystallographic artifact as was previously established [1, 3].

Based on the above-mentioned data some important questions have arisen. First, it is not clear whether an antagonist conformation of H12 in PPAR γ could exist at all, and if not, what

might be the reason for this difference compared to many other NRs. Second, it is questionable whether the small conformational changes observed by the regular cMD simulations are due to an inadequate sampling or the existing antagonist classes are just not capable of fully transforming the H12 to an antagonist conformation. If the latter is true, it is also important to propose a guide for a new ligand substructure targeting. Finally, there should be revealed the actual reason for the different H12 conformation in chains A and B, in most of the PPAR γ X-ray structures.

The advanced MD techniques including aMD and metadynamics, provide a helpful tool for studying the structural and dynamical properties of the receptor at a sub-millisecond time scale, and together with the much better sampling would help to determine the most populated H12 conformations in its apo form.

In the current work we performed a high-throughput MD study and sampled the H12 conformational space in the PPAR γ apo form by aMD and metadynamics, describing the most likely activation helix conformations in both a monomer and a homodimer configuration. The H12 conformation in the holo form of the receptor, when it is bound to an antagonist, is also revealed. Based on the obtained results, an explanation about the observed asymmetry in most of the PPAR γ crystal structures was provided. The protein substructures to be targeted by ligands, in order to achieve a stable antagonist receptor form, were identified.

2. Results and Discussion

2.1 H12 conformation in the holo PPAR γ receptor bound to an antagonist

Initially, we investigated the holo PPAR γ form, to determine the most likely conformations of H12 when the receptor is in a complex with the recently discovered PPAR γ non-covalent full antagonist (ligand 9p ref [7]). Two independent aMD simulations of 500 ns were performed. The original hypothesis of the developers of this ligand was that the compound would act as a typical NR antagonist, pushing away H12, in particular Tyr473, and transforming it into an antagonist orientation. However, we did not observe such a dramatic conformational change, presumably, due to the detected mutable binding modes of this ligand (see video S1). These results agree with our previous cMDs. The aMD simulations described mutable ligand binding modes and a sample of diverse H12 states, some of which can accommodate co-repressors. The obtained averaged conformation was similar to its full agonist state (RMSD of about 2 Å). Thus, this is a strong indication that the observed H12 conformational changes in the holo receptor form that is liganded with this class of non-covalent full antagonists, is not a

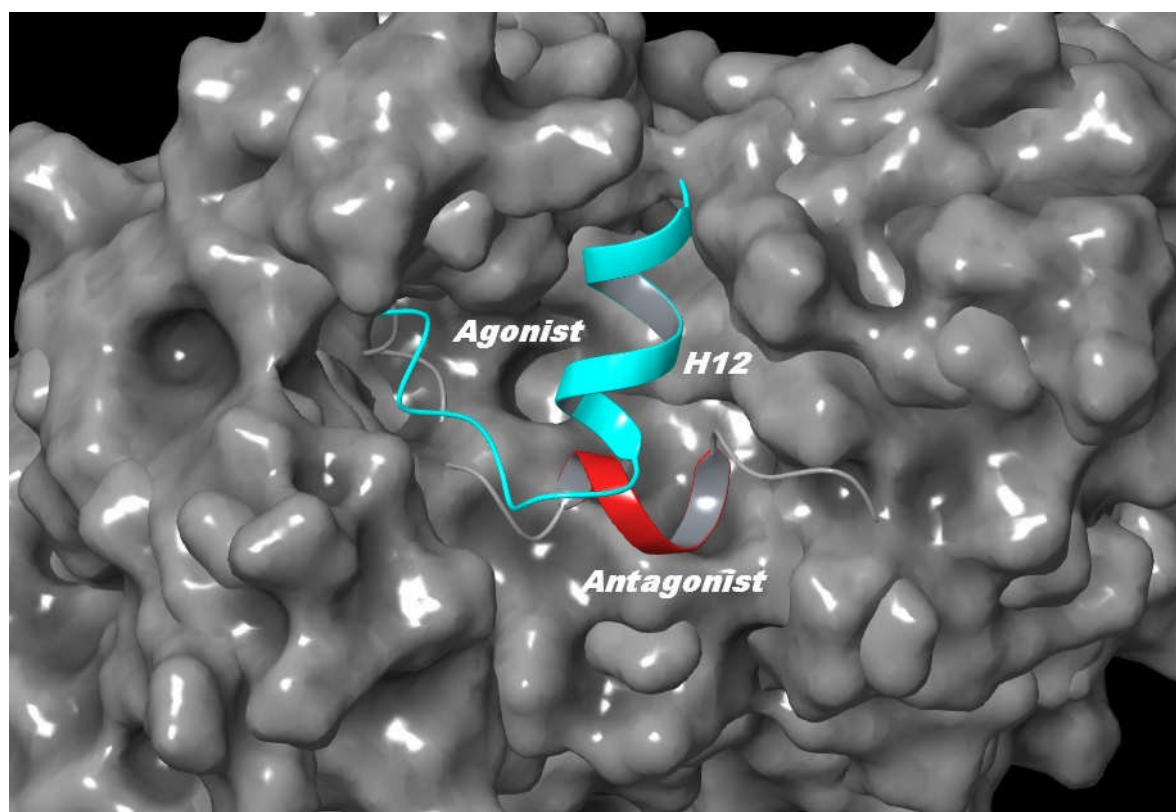


Figure 1. Observed helix 12 (H12) antagonist conformation in a PPAR γ monomer, based on the corresponding representative cluster collected by all aMD simulations (in red colour). For comparison, the full agonist state obtained by the same simulations is presented (in sky blue colour).

sampling problem. Such compounds may not fully transform H12 to an antagonist state as it is observed in the PPAR α . Therefore, we dare to predict that ligands are still to be synthesized favoring the full antagonist H12 position, and a corresponding X-ray structure can be resolved. Detailed results of this study are presented in an individual paper [8].

2.2 X-ray observed H12 conformation in Chain B is an artifact

Further, we investigated whether the observed in most X-ray structures H12 inclined conformation in chain B is well populated in the apo monomer receptor form and thus can be stabilized by some specific type of ligand-receptor interactions that reshapes the activation helix free energy landscape. Six 400-ns-long independent aMD simulations with high dual boost potentials have been employed (see Methods part). This aggressive acceleration may increase the noise produced, affecting both the population and the free energies estimations, but it does not have an impact on the presence of one or another conformational state. The data obtained have clearly demonstrated that the X-ray resolved inclined H12 conformation is not populated at all, hence not likely, and the activation helix adopts in a short time (3-20 ns)

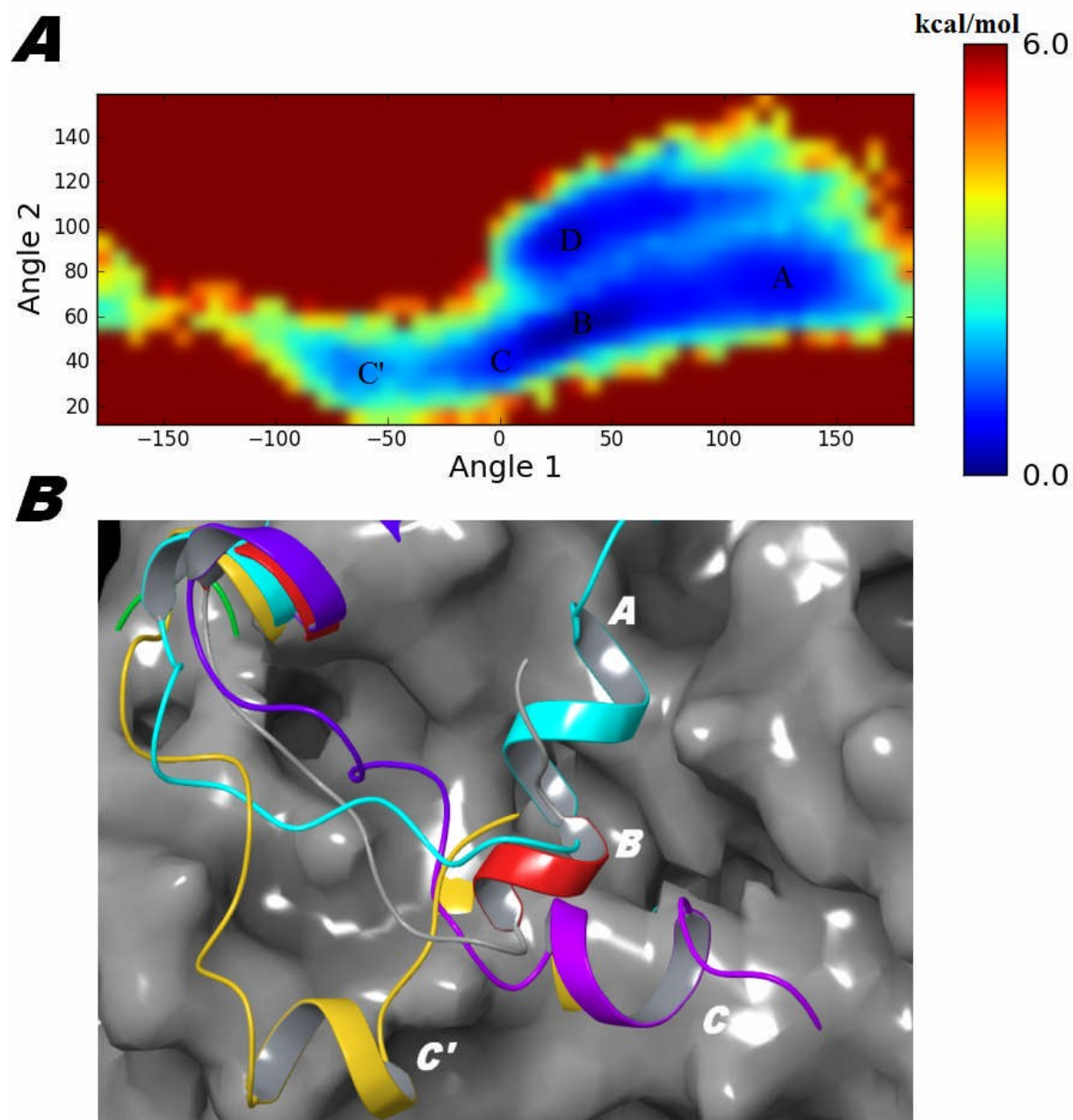


Figure 2. (A) Reweighted free energy plot created by the combined values, from all aMD simulations in a monomer, using angles 1 and 2 as coordinates. The most populated conformational states of H12 are indicated as follows: Point A is a full agonist, point B is an inclined metastable conformation toward H4, point C represents the antagonist state, which is divided into two well evident sub-clusters (C and C'), and point D is an unattached H12 conformation. (B) Structural representation of the detected H12 clusters of conformations. The H12 conformation distant from LBD (point D) was omitted for clarity.

a conformation close to the LBD, initially resembling its full agonist position. Moreover, the average structure obtained by these aMD runs has shown H12 in a different orientation than those seen in X-ray data. Nevertheless, the main result from these simulations has been the notable finding that the H12 of PPAR γ adopts an antagonist-like conformation, named in short here as antagonist, similarly to other nuclear receptors including ER α and PPAR α . Such

a conformation was present and well populated in all of the performed simulations. However, the number of the H12 residues resolved in chain B (pdb id 3vso structure), used for these simulations, is smaller than those crystallized in chain A. Thus, initially we decided that this was an artifact from the system setup and consequently built up a new monomer structure with a H12 length that is equal to chain A (see Methods).

2.3 Monomer specific H12 conformations

Further, a series of ten 500-ns-long aMD runs with lower boost potentials were performed. Eight of the total ten runs confirmed that the H12 antagonist conformation exists and is also well populated in PPAR γ (see Figure 1 and video S2). To illustrate the changes in the H12 conformation and estimate the weight of the different populations, reweighted free energy maps were created, using two selected angles as coordinates that describe the activation helix orientation in a simple way. The dihedral angle between the C α atoms of Ile472, Leu468, Gln286 and Val290 (Angle 1) was chosen to represent the H12 position in relation to H3, whereas the angle between Leu468, Ile472 and Gln454 (Angle 2) represented the orientation toward the H11 (see Figures S1A and S1B). The two well visible blue stripes on Figure 2A reflect the H12 flexibility in two distinguished regions. The first one is a conformation that is relatively unattached but still close to the LBD, and the second one is that in which H12 binds in the LBD cleft in either an agonist or an antagonist state. Several discrete conformations are well visible within these regions, which seem to also have similar free energies (1-2 kcal/mol differences). It should be noted that the free energies obtained by the existing aMD reweighting schemes in a protein with such a size may suffer from serious deviations, but this currently highly disputable topic is outside the scope of this paper [12-13]. Nevertheless, the most populated activation helix conformation (point B on Figure 2A) is the one inclined by about 15 degrees forward to helix 4 (H4) (see Figure 2B). The full agonist conformation (point A) is populated similarly to those of the antagonist state (point C). In addition, a more prolonged antagonistic conformation, like those seen in PPAR α , is also present (point C'). The H12 conformations cluster that is outside the LBD, resembling its full agonist position, is presented too (point D). The comparable populations of the antagonist and agonist states resemble those obtained for the estrogen receptor alpha (ER α) by both the HDX and the aMD approaches [14-15].

To gain a more detailed and plausible insight into the free energies of individual H12 conformational states series of well-tempered metadynamics simulations (WT-MetaD) of the PPAR γ monomer were also executed. For these runs we used more simple description of the

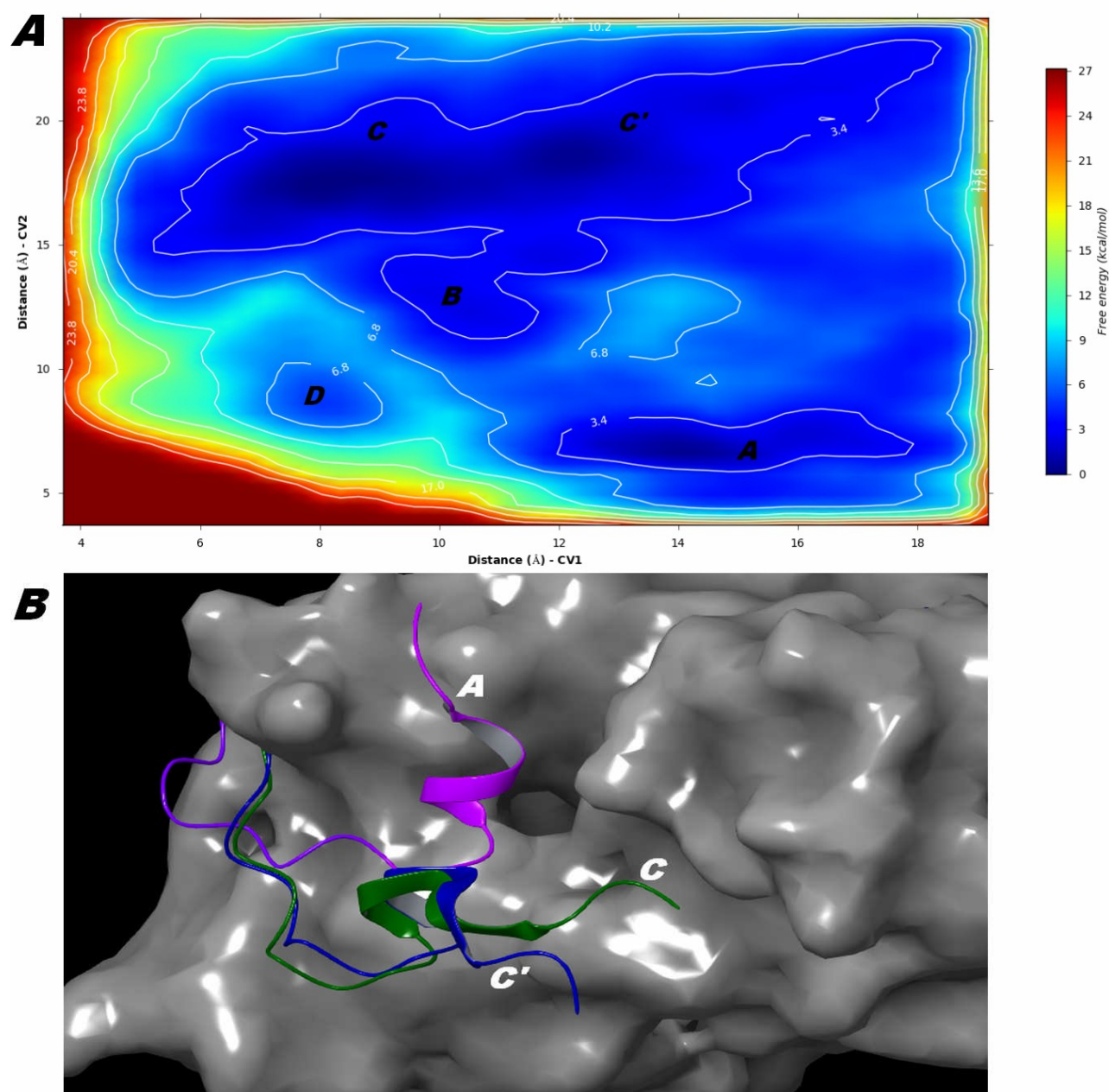


Figure 3. (A) Free energy plot obtained by well tempered metadynamics simulations in a monomer, using distances 1 and 2 as CVs (see text). The free energy minimum designations are the same as those indicated on Figure 2. (B) Structural representation of the detected H12 clusters of conformations. The conformations that represent points B and D were omitted for clarity and are similar to those retrieved by aMD simulations.

activation helix position. The distances between the $C\alpha$ atoms of H12's Tyr473 and the residue Lys319 in H4 (distance 1, CV_1) and Leu453 in H11 (distance 2, CV_2) were selected as collective variables (CVs), respectively. After the adjustment of the parameters (see Methods), three independent 100-ns-long WT-MetaD runs were executed. Metadynamics simulations

confirmed the presence of an antagonist state and also described the likely H12 conformations (see Figures 3A and 3B). Notably, the WT-MetaD runs detected the same specific conformations inside the main clusters, as for example the full agonist state, as they were also captured by our current and previous cMDs [5]. It is also important to note that these similar results were achieved not only by individual techniques but also by different force fields. The aMD simulations were performed using Amber14SB, whereas the metadynamics by the new OPLS3 field. However, the difference between these approaches was the shape of the detected H12 antagonist conformation. The aMD runs have indicated that the activation helix is more helical, whereas the metadynamics simulations have indicated that it is in an unfolded and much more flexible configuration, resembling those observed in PPAR α , thus opening the pocket for co-repressor binding (see Figure S2). These results are not unexpected as it has recently been shown that simulations using Amber SB force field reproduce more helical structures than those using OPLS (see Methods). We presume that the real H12 conformation in an antagonist form is somewhat median between the observed conformations by these force fields.

Surprisingly, antagonists (points C and C') and agonist (point A) states revealed virtually the identical free energy ($\Delta G=0.5$ kcal/mol) The lowest energy was those of conformation C (see Figure 3A). The H12 configuration between the agonist and antagonist states oriented toward H4 (point B) had a value of $\Delta G=2.4$ kcal/mol. The detached H12 state (point D) showed an energy difference of 4.7 kcal/mol whereas the inclined X-ray conformation in chain B was separated by an energy barrier higher than 10 kcal/mol; hence both of them can be considered as unlikely configurations. According to Figures 2A and 3A the transition between the agonist and antagonist states occurs via an intermediate metastable state (point B). However, the metadynamics results allow not only to calculate the difference between free energy minimums but also to assess the height of the free energy barriers between these conformations thus providing also an idea about the transition rates. The energy barriers between the antagonist (point A), the intermediate (point B) and agonist (point C) states are 4.2 and 5.9 kcal/mol, respectively(see Figure 4A). These data indicate that the transition rate between the agonist and antagonist is within an order of nanoseconds and thus, similarly to other NRs [4, 14], a fast exchange between these states is present. Further, it is evident that the transition between the lowest energy states passes via barriers that define the intermediate H12 conformation (point B) as relatively stable. Based on these results one can suggest that the existing non-covalent antagonists stabilize the receptor in this intermediate metastable

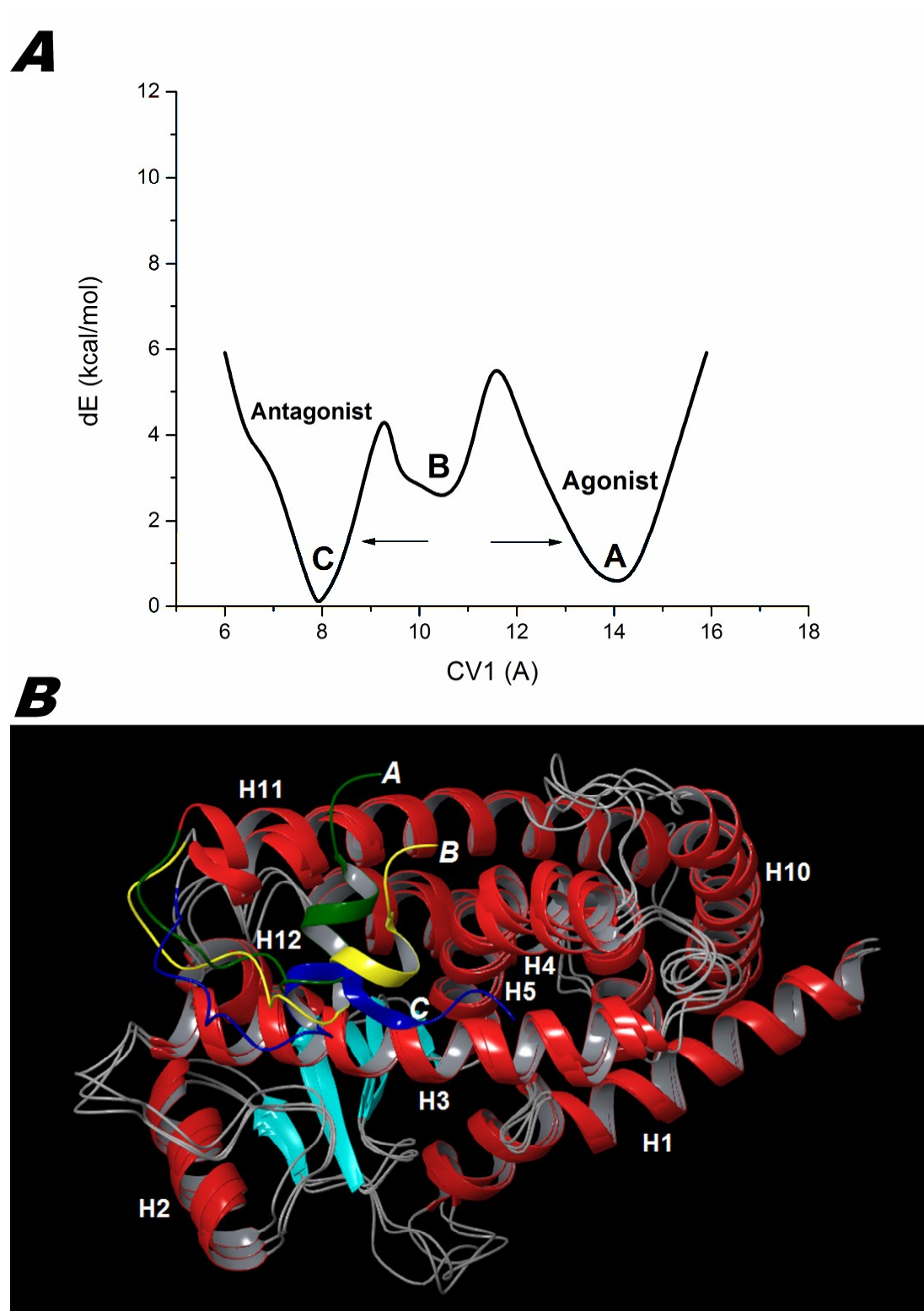


Figure 4. (A) Transition path between agonist (point A), the intermediate (point B) and antagonist (point C) states. (B) Structural representation of detected three lower energy conformational states.

state. This suggestion could explain why these antagonists can not fully transform PPAR γ in an antagonist form. Finally, from the free energy/population graphics it is apparent that the ensembles of antagonist states (C plus C') are better pronounced compared to the agonist ones.

This result agrees well with the experimental data which show that in the apo form the receptor binds predominantly co-repressors and, in much less extent, but notably, also co-activators [1-4]. The structural features of the whole receptor in the above-mentioned states are present on Figure 4B.

2.4 Detected H12 conformations in a dimer

Finally, based on our previous results which indicated that dimerization had a leading role in the H12 conformation in the ER α receptor [15], and those very recently obtained by several experimental techniques for both the TR-RXR α and PPAR γ -RXR α complexes [16], we performed 10 independent 400-ns-long aMD simulations on a PPAR γ homodimer. We did not use the physiological complex with RXR α because the aim of the studies was to determine the role of the PPAR γ homodimer in the H12 orientation as seen in the X-ray structures. However, it should be noted that PPAR γ form a strong homodimer *in vitro* that has also been able to bind coactivators [17]. Moreover, similar binding affinities have been measured when a coactivator is bound to either PPAR γ -RXR α heterodimer or PPAR γ homodimer and the prevalence of the PPAR γ -RXR α complex formation *in vivo* has been revealed and discussed [17].

As a result, we confirmed that the PPAR γ H12 conformation was also mediated by the protein-protein interactions. Similarly to the ER α , the H12 in one of the homodimer units was stabilized and was mainly in an identical to the full agonist state folding but in the second one it was unstable (see Figures 2A, 5A and 5B). The altered receptor dynamics in the individual dimer chains were initially indicated by the deviated values of Angle 2, which reflected the H11 change in the orientation due to the interactions with the same helix in the second homodimer unit. The last angle was shifted by about 20 degrees, thus an angle of 50 degrees in a monomer corresponded to 70 degrees in a dimer (see Figures 2A and 5A). The Angle 1 describing H12 position toward H3 was unchanged. A similar deviation was also observed in the second dimer chain but the deviation in the Angle 2 was only about 10 degrees (see Figure 5B). The most visible result from these free energy maps was that the activation helix ensemble of conformations was completely different in chains A and B. Chain A was populated with several fluctuating states that were similar to the full agonist conformation. For instance, point A'' on Figure 5A represents the H12 state as visible in most X-ray structures, i.e. the full agonist orientation, whereas the points A and A' are activation helix conformations that exhibited a slightly inclined position toward H4 and H11, respectively. On

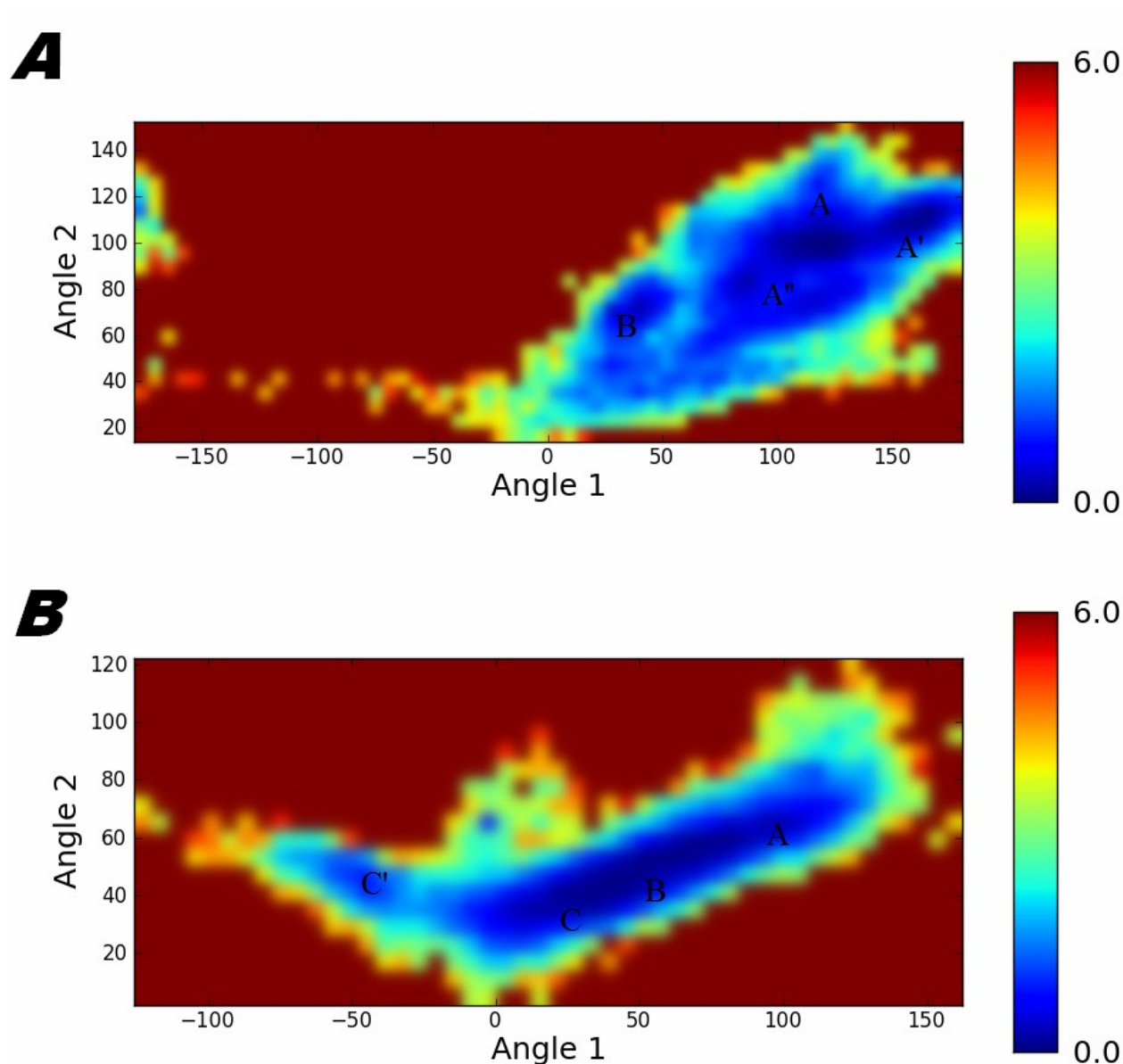


Figure 5. Reweighted free energy plots created by the combined values, from all aMD simulations in a dimer, (**A**) chain A and (**B**) chain B, using the angles 1 and 2 as coordinates. The most populated conformational states of H12 are identical to those on Figure 2 and are indicated with the same symbols. Point A'' on Figure 5A corresponds to the crystallographic full agonist H12 position. Note that the angles 1 and 2 were shifted by 10 and 20 degrees compared to that in the monomer, respectively.

the other hand, H12 states in chain B (points A-C and C') were similar to those described in a monomer (see Figures 2A and 5B). However, in the homodimer there were no unattached H12 positions, which is an indication of the helix 12 stabilization in a dimer. The fact that different ensembles were observed in identical subunits, but at the same time a reasonable convergence was achieved during a number of simulations, is a direct indication that long-

range interactions between chains are also a significant factor for the H12 conformation (see also the discussion below).

2.5 Structural properties of H12 in a dimer

If the results above are indicative of the dissimilarities in the dynamics between individual homodimer units, it is also interesting to trace how these alterations impact on the medial aMD structures and how they compare to the available X-ray data. Our analysis showed that the averaged over generated aMD ensembles H12 structure in the first homodimer unit had almost completely overlapped the one seen in the crystallographically resolved chain A (RMSD of only 0.8 Å). Also, even the loop between H11 and H12 was with a very similar conformation, further confirming that aMD simulations reproduced in a good way the experimental data (see Figure S3). Note that the initial H12 conformation in both dimer components was reconstructed based only on the X-ray chain B structure where H12 was detached from LBD. On the contrary, in the second homodimer unit, H12 behaved as in a monomer, and the presence of an antagonist state was even more evident, leading to an average orientation which was more inclined toward H4 activation helix (see Figure S4). Compositions of two independent 200-ns-long conventional dynamics on a monomer and 400-ns-long on a dimer were also executed, but they described only the H12 conformation detached from LBD, i.e. those seen in the X-ray structure, thus explaining why previous cMD simulations failed to describe more likely activation helix states (see Figure S5). In both the monomer and the dimer the antagonist H12 conformation was stabilized by an H-bond network between Lys319 and the backbone oxygen of Tyr473 and Lys474, and also the hydrophobic contacts of residues Leu468, Ile472 and Tyr473 (see Figure S6A). The well known and significant for the ligand binding residues His323, His476 and Tyr327 in the LBD were unchanged compared to those seen in chain A and in the structures retrieved by the above-mentioned cMDs, thus they were in a configuration ready to accommodate a ligand [5]. The identified contacts for the detected lower energy states and the whole dimer structure in an antagonist form are present on Figures S6B-S6D.

Based on the obtained results, it can be predicted what type of ligands should be developed in order to be achieve an antagonistic receptor form. The simple alignment of the PPAR γ antagonist structure retrieved here and those obtained by X-ray technique for the structurally similar analog PPAR α (Figure S2) indicates that both receptors have a similar H12 conformation. Thus, considering also the sequence similarity between these receptors and that the bottom of H12 was the primary ligands target in PPAR α , it might be expected that the

antagonistic PPAR γ conformation can be achieved in a similar manner, i.e. via destabilization of Leu465 and Leu469. Simultaneously targeting of Tyr473 (H12) and Gln286 (H3) are most likely also required.

Notably, the average structures of both the monomer and the second homodimer unit showed a H12 conformation that was similar to those of chain B in the X-ray data (see Figure S4) but without such a degree of similarity as those seen in chain A (Figure S3). Indeed, an easy interpretation of these results would be that our simulations reproduced in a reasonable way the H12 conformations in both chains of the apo structure pdb id 1pgr. However, most of the liganded PPAR γ resolved complexes have almost the same conformations of H12 in their chains B, too. Besides, the authors of the above-mentioned apo structure have proposed that this activation helix orientation is due to the interaction with a third monomer and is likely a crystallographic artifact [17]. Thus, our data simply indicate that the provoked instability in chain B lead to an exchange between the agonist and the antagonist states, predisposing H12 to be eventually more affected by another monomer structure during the crystal packing but also by a different type of ligands. On the other hand, the activation helix conformation does not seem to be different in the presence of various partial agonists. Hence, based on these results, we suggest that the initial hypothesis about the crystal packing contribution to the H12 conformation in chain B should be revised because it is evident that more complex processes are present in the second homodimer unit. The ligand phenotype – H12 orientation theory should be refined too

Our data suggest that the averaged structures obtained by the large set of aMD generated H12 ensembles represent the effect of long-range interactions occurring between both chains A and B and that they themselves can be responsible for the H12 asymmetry. On the other hand, the simulations have clearly shown that the conformation observed in the X-ray structures is not achievable in a solution. Thus the initial hypothesis of the 3rd monomer role during the crystal packing and H12 conformation seems to be reasonable but can be considered as an additional factor for the naturally occurred asymmetry due to the long-range interactions. In other words, the role of the 3rd monomer unit is just to change the free energy landscape and H12 stabilization in the conformation observed in most X-ray structures. In some PPAR γ X-ray structures, where a strong agonist was bound, H12 was in an identical to a full agonist conformation in both chains, which further supports our data and indicates that the asymmetry can be abolished by strong activation helix stabilization. The latter also supports the concept of the ligand phenotype - H12 orientation hypothesis, but both crystallography and our data

indicate that the interactions with the 3rd monomer have a predominate role, which disguises the H12 conformational effect of the variations in partial agonist structures.

The set of all performed aMD simulations have shown an exchange of the homodimer unit where H12 is in a stable agonist form, which indicates that the initial stabilization in one of the chains leads to destabilization in the second one. This is an interesting event that has been already observed both theoretically and experimentally in ER α [14-15] and also recently in PPAR γ [16]. The source of these differences was similar to those observed in an ER α homodimer [15] where the interactions between the pair of H11s were transmitted to the H5 and from there to the H12 (data not shown). In fact, a very recent multi experimental study has confirmed both our previous and present aMD results [16], showing that an allosteric signaling pathway occurs exactly through a sequence of conformational relays between the helix 11 pairs that constitute most of the dimer interface, transferred to a rotation of helix 5, leading to a disruption of the adjacent co-regulator and ligand-binding sites. Thus it seems that such mechanism is likely to be common for many NRs.

2.6 Comparison of experimental data and convergence of the simulations

It should be underlined that a direct comparison of the results obtained here is difficult to perform based on the available experimental data due to the high H12 flexibility in the apo receptor and the lack of appropriate antagonist ligands that can transform the activation helix in an antagonist form. However, the reproduction of the agonist H12 state was a useful way to compare our results to the experimental data. Besides, the H12 flexibility observed in the aMD simulations agrees well with many previous studies where it was already described in details [1-3]. Moreover, during all simulations, we also observed a highly dynamic behavior of the H3 central part centered at Ala291. This indirectly concurs with both NMR and HDX data, which revealed that this receptor region is the most stabilized upon ligand binding [1-3]. The direct comparison of the antagonist state obtained here with those observed in PPAR α (pdb id: 1kkq) is considered by us as an impractical approach because this complex was solved with an antagonist ligand and a co-repressor, which would reshape the free energy landscape and displace the activation helix in a different conformation, i.e. energy minimum. Moreover, in a contrast to the agonist state, the antagonist conformation significantly varies between NRs (see pdb ids 1kkq (PPAR α) and 3ert (ER α) for comparison). Therefore, it is also possible to expect a variation in the antagonist configurations. However, the secondary cluster of the H12 antagonistic conformations obtained by aMD runs (point C') and also those retrieved by metadynamics simulations resembled well the antagonistic PPAR α activation

helix state. This cluster was separated, according to the metadynamics, by only 0.5 kcal/mol energy barrier and the flexibility of the last part of H12 opening the binding pocket for co-repressor adoption (see Figure S2).

To further support the reliability of the obtained results, we also performed rigorous analyses of the simulations convergence. The convergence analyses of the individual aMD simulations were performed via RMS average correlations (RAC) and Kullback–Leibler divergence (KLD) methods [18-19] (see SI methods). Metadynamics convergence was monitored too. The simulations converged reasonably, thus describing plausibly the receptor conformational space (see Figures S7-S11 and the corresponding SI methods part). The intra simulations convergence, i.e. the reproducibility between the different simulations, is also important. An example for good convergence of the whole receptor structure between the aMD runs were aMD7 and aMD8 simulations on a dimer (see Figure S9), whereas an example for poor convergence was found between aMD2 and aMD10 runs (see Figure S10).

3. Conclusions

The main finding from our relatively long simulations is the presence of an antagonist H12 conformation, which presumably can be detected experimentally when an appropriate non-covalent antagonist would be designed and bound to the receptor. Moreover, our data provide clear evidence that the activation helix adopts a conformation, which opens the LBD for a ligand binding path that is blocked in H12 full agonist state. Our *in silico* study would lead to the development of such non-covalent antagonists and/or the introduction of point mutations at the bottom of H12, which would change the free energy equilibrium to an antagonist conformation and thus both the dynamics and the PPAR γ structure in an antagonist state would be experimentally confirmed. The urgent need of such an antagonist development with pharmaceutical application has been recently recognized [7], adding yet more significance to the reported here results.

4. Methods

4.1 Protein structure preparation

The X-ray structure of the PPAR γ in a complex with the ligand MEKT-21 (pdb id 3vso) was employed as a starting model. This choice was motivated due to the fact that above-mentioned structure was used as a template for the design of the initially investigated complex of the liganded with the antagonist 9p receptor form [7] (see video S1). Further, this structure was

also used for the current study of the apo system constitution. Only chain B, where the helix 12 conformation is detached from its full agonist binding pocket, was chosen for all simulations. However, the H12 length in chain B solved in most of the X-ray structures is shorter than those in chain A. To add the missing residues, we used as a template the structures where both chains had an equivalent number of residues. Simulations of a monomer with both variants of H12 length were performed (see below). The homodimer structure was created by aligning the constructed chain B (with the longer H12 variant) on the X-ray chain A, in order to have detached from LBD H12 states in both homodimer units.

The protein structure was initially prepared by the Protein preparation wizard module of the Schrödinger 2015-2 software [20]. All settings were set to defaults. A truncated octahedral of TIP3P water molecules, 10 Å dimension in each direction and counterions were added by AmberTools 15 suite [21] to obtain the final solvated system, which consisted of nearly 43 000 and 86 000 atoms for the monomer and dimer, respectively.

4.2 Conventional molecular dynamics (cMD)

Conventional molecular dynamics (cMD) was carried out using the Amber 14 program and the Amber14SB force field [21]. Initially, the systems were energy-minimized in two steps. First, only the water molecules and ions were minimized in 6000 steps while keeping the protein structure restricted by weak harmonic constrains of $2 \text{ kcal mol}^{-1} \text{ \AA}^{-2}$. Second, a 6000 steps minimization with the conjugate gradient method on the whole system was performed. Furthermore, the simulated systems were gradually heated from 0 to 310 K for 50 ps (NVT ensemble) and equilibrated for 3 ns (NPT ensemble). The production runs were performed at 310 K in a NPT ensemble. Temperature regulation was done using a by Langevin thermostat with a collision frequency of 2 ps^{-1} . The time step of the simulations was 2 fs with a nonbonded cutoff of 9 Å using the SHAKE algorithm [22] and the particle-mesh Ewald method [23]. An initial 30-ns-long equilibration simulation was executed. Two independent 200-ns-long cMD simulations of a monomer and also 400 ns long production runs on a homodimer were finally performed.

4.3 Accelerated molecular dynamics (aMD)

The accelerated molecular dynamics (aMD) simulations provide the possibility to sample the conformational space much better and to detect the local energy minima that remain hidden in the cMD calculations [24-25]. Moreover, aMD simulations can boost the sampling by up to 2000 times compared to cMD [24]. Thus, one can consider that the sampling performed by a

500 ns aMD trajectory might be equal to that of hundreds of microseconds of cMD simulation. aMD modifies the energy landscape by adding a boost potential $\Delta V(r)$ to the original potential energy surface when $V(r)$ is below a predefined energy level E :

$$\Delta V(r) = \begin{cases} 0, & V(r) \geq E \\ \frac{(E - V(r))^2}{\alpha + (E - V(r))} & V(r) < E \end{cases} \quad (1)$$

In general, this approach also allows the correct canonical average of an observable calculated from configurations sampled and the modified potential energy surface to be fully recovered [12-13].

All of the aMD calculations were performed using the Amber 14 molecular modeling package and the Amber14SB force field [21]. The production runs were performed at 310 K in a NPT ensemble. A mentioned above 30-ns-long equilibrated run by cMD system was used as an input for all the performed MD simulations. Temperature regulation was done using a Langevin thermostat with a collision frequency of 2 ps^{-1} . The time step of the simulations was 2 fs with a nonbonded cutoff of 9 Å using the SHAKE algorithm [22] and the particle-mesh Ewald method [23].

In order to simultaneously enhance the sampling of the internal and diffusive degrees of freedom, a dual-boosting approach based on separate dihedral and total boost potentials was employed [12, 24-25]. This method may be compromised by the increased statistical noise but was also successfully applied in similar studies [15, 24]. The selections of the boost parameters E and α for the dihedral boost and the total boost were based on the corresponding average dihedral energy and total potential energy obtained from combined and the above-mentioned cMD production runs (2x200ns for the monomer and 2x400 ns for the homodimer, respectively). For most simulations in both the monomer and the homodimer, the dihedral boost parameter, E_d , was set equal to the average dihedral energy obtained from the cMD simulation plus $N_{\text{sr}} \times 3.5 \text{ kcal/mol}$, where N_{sr} is the number of solute residues; the α_h parameter was then set equal to $E_d/5$. For the total boost parameter, E_p , the value was set to be equal to $0.20 N_p$ plus the average total potential energy obtained from the cMD simulation, where N_{tot} was the total number of atoms; α_{tot} was simply set equal to $0.2 N_{\text{tot}}$. Thus the $\alpha_h=3.5$, $E_h=0.2$, $\alpha_p=3.5$ and $E_p=0.2$ were employed. However, for some simulations of a monomer more forceful boosts were also chosen: $\alpha_h=4.0$, $E_h=0.3$, $\alpha_p=4.0$ and $E_p=0.3$ (see Results and discussion). Six independent production aMD runs were initially performed by the last aggressive boosts parameters on a monomer with an equivalent to X-ray chain B H12 residues

number (the shorter in length H12 variant in our setup). Further, they were followed by execution of ten independent 500-ns-long aMD simulations of a monomer with the lower boosts mentioned above and longer H12. Finally, for the H12 description in a dimer ten 400-ns-long aMD runs were executed. All analyses were performed on the combined trajectories from these simulations.

Reweighting of biased aMD frames is an important procedure and was performed based on the Maclaurin series expansion scheme up to the order of the 10th. This is a highly disputable topic [13], which is described in details in the corresponding SI Methods section. It should be noted that all free energy maps are based on the obtained populations as discussed in SI Methods. On the free energy plots, the dihedral angle between the C α atoms of Ile472, Leu468, Gln286 and Val290 (Angle 1) was chosen to represent the H12 position in relation to H3, whereas the angle between Leu468, Ile472 and Gln454 (Angle 2) the orientation toward the H11.

Finally, convergence analyses were performed by the RMS average correlations method (RAC) [18] and the Kullback–Leibler divergence (KLD) [19] (see SI Methods for more details).

4.4 Metadynamics

Metadynamics is a powerful algorithm that can be used both for reconstructing the free energy and for accelerating rare events in systems described by complex Hamiltonians. Similar to the aMD method, in metadynamics, the potential energy landscape is modified. However, instead of modifying the potential energy of the entire system, in this method the focus is only on the configurational space of relevant, manually chosen collective variables (CVs), described by differentiable functions of Cartesian coordinates of atoms. Motion of the system along these variables can be accelerated by adding an artificial Gaussian-shaped bias potential to the energy in CV space in each step, to discourage the system from revisiting previously visited states [26]. In our simulations, we employed well-Tempered Metadynamics, which guarantees the theoretical convergence of the simulation, by rescaling the Gaussian weight factor during the simulations so that smaller biases are added as the simulation progresses, was employed in this work [27].

The WT-MetaD was performed by Desmond package included in the Schrodinger 2015-2 suite and the newly developed OPLS3 force field (FF) was employed [20]. The choice of an OPLS FF was due to the well known fact and recently published results that even after the "SB" modifications the simulations by Amber and FF produce more helical structures than the

OPLS FF [28-30]. Moreover, this FF have clearly shown that it is much superior than the previous OPLS FF generations and thus it deserve a case study [31]. The choice of collective variables (CVs) is a critical step in the metadynamics calculations. We did not use the same angles that were employed for the aMD free energy landscape visualization because they were simply not sufficient choice as CVs for metadynamics calculations and most of the runs even crashed during the first nanoseconds of the simulations. Moreover, these angles were chosen only because they have illustrated the registered by aMD free energy minimums better. Instead, the distances between the C α atoms of H12's Tyr473 and the residue Lys319 in H4 (distance 1, CV₁) and Leu453 in H11 (distance 2, CV₂) were selected as collective variables (CVs), respectively. Several 50-ns-long WT-MetaD simulations were executed to adjust the parameter sets for the selected CVs in a way to provide a good convergence and description of the individual H12 states. For instance, a Gaussian height of 0.15 kcal/mol was initially used. However, adding this or a lower value took about 25 ns of the simulation time in which only the interactions with H3 to be overcome and the activation helix to adopt an agonist conformation in the LBD, i.e. only the low populated and presumably unphysical states were mainly described (see Results and discussion paragraph). Although presumably more precise results can be obtained by this lower boosts, this would take a lot of time for the H12 conformational landscape sampling.

The final parameters for all production runs were: Gaussian height of 0.4 kcal/mol, width of 0.25 Å and 2 ps interval at which the repulsive Gaussian potential is added, respectively. A constant of $kT=5.0$ kcal/mol was set for the WT-MetaDs. These values described also in the best way the well known full agonist state and the specific structural variations, such as for example the Tyr473 conformations, retrieved by NMR data and cMD simulations [1-3, 5]. Three independent 100-ns-long simulations were performed for the production runs. The convergence was estimated in two different ways. First, we split each performed simulation in three individual portions of 40, 70 and 100 ns trajectories, respectively. Further, we investigated in the same way all of the independent runs. No significant free energy variations were observed between the 70 and 100-ns-long simulation period (see Figure S11). All independent runs provided virtually the same results and the free energy deviations in the detected minimums were no more 0.5 kcal/mol.

Acknowledgements

Thanks due to Prof. Anny Usheva (Harvard Medicinal School) for editing the manuscript and the helpful discussion. We thank also to Maya Marinova for editing the manuscript and to

Ivanka Tsakovska and Prof. Ilza Pajeva (Bulgarian Academy of Sciences) for the helpful suggestions.

References

- [1] J. B. Bruning, M. J. Chalmers, S. Prasad, S. A. Busby, T. M. Kamenecka, Y. He, K. W. Nettles and P. R. Griffin, Partial agonists activate PPAR γ using a helix 12 independent mechanism, *Structure*, 2007, **15**, 1258–1271.
- [2] Y. Hamuro, S. J. Coales, J. A. Morrow, K. S. Molnar, S. J. Tuske, M. R. Southern and P. R. Griffin, Hydrogen/deuterium-exchange (H/D-Ex) of PPAR γ LBD in the presence of various modulators, *Protein Sci.*, 2006, **15**, 1883–1892.
- [3] T. S. Hughes, M. J. Chalmers, S. Novick, D. S. Kuruvilla, M. R. Chang, T. M. Kamenecka, M. Rance, B. A. Johnson, T. P. Burris and P. R. Griffin, Ligand and receptor dynamics contribute to the mechanism of graded PPAR γ agonism, *Structure*, 2012, **20**, 139–150.
- [4] M. R. Batista and L. Martínez, Dynamics of nuclear receptor Helix-12 switch of transcription activation by modeling time-resolved fluorescence anisotropy decays, *Biophys. J.*, 2013, **105**, 1670–1680.
- [5] F. Fratev, I. Tsakovska, M. Al Sharif, E. Mihaylova and I. Pajeva, Structural and Dynamical Insight into PPAR γ Antagonism: In Silico Study of the Ligand-Receptor Interactions of Non-Covalent Antagonists, *Int. J. Mol. Sci.*, 2015, **16**, 15405-15424.
- [6] H. E. Xu, T. B. Stanley, V. G. Montana, M. H. Lambert, B. G. Shearer, J. E. Cobb, D. D. McKee, C. M. Galardi, K. D. Plunket, R. T. Nolte, D. J. Parks, J. T. Moore, S. A. Kliewer, T. M. Willson and J. B. Stimmel, Structural basis for antagonist-mediated recruitment of nuclear co-repressors by PPAR α , *Nature*, 2002, **415**, 813-817.
- [7] M. Ohashi, K. Gamo, Y. Tanaka, M. Waki, Y. Beniyama, K. Matsuno, J. Wada, M. Tenta, J. Eguchi and M. Makishima, Structural design and synthesis of arylalkynyl amide-type peroxisome proliferator-activated receptor γ (PPAR γ)-selective antagonists based on the helix12-folding inhibition hypothesis, *Eur. J. Med. Chem.*, 2015, **90**, 53–67.
- [8] F. Fratev, PPAR γ non-covalent antagonists exhibit mutable binding modes with a similar free energy of binding: A case study, *J. Biomol. Struct. Dyn.*, 2016, DOI: 10.1080/07391102.2016.1151830.
- [9] M. Ohashi, K. Gamo, T. Oyama and H. Miyachi, Peroxisome proliferator-activated receptor gamma (PPAR γ) has multiple binding points that accommodate ligands in various

conformations: Structurally similar PPAR γ partial agonists bind to PPAR γ LBD in different conformations, *Bioorg. Med. Chem. Lett.*, 2015, **25**, 2758-2762.

[10] T. Itoh, L. Fairall, K. Amin, Y. Inaba, A. Szanto, B. L. Balint, L. Nagy, K. Yamamoto and J. W. Schwabe, Structural basis for the activation of PPAR γ by oxidized fatty acids, *Nat. Struct. Mol. Biol.*, 2008, **9**, 924-931.

[11] V. A. Dixit and P. V. Bharatam, SAR and computer-aided drug design approaches in the discovery of peroxisome proliferator-activated receptor γ activators: A perspective, *J. Comput. Med.*, 2013, 406049.

[12] Y. Miao, W. Sinko, L. Pierce, D. Bucher, R. C. Walker and J. A. McCammon, Improved Reweighting of Accelerated Molecular Dynamics Simulations for Free Energy Calculation, *J. Chem. Theory Comput.*, 2014, **10**, 2677-2689.

[13] Z. Jing and H. Sun, A Comment on the Reweighting Method for Accelerated Molecular Dynamics Simulations, *J. Chem. Theory Comput.*, 2015, **11**, 2395–2397.

[14] S. Y. Dai, M. J. Chalmers and J. Bruning, Prediction of the tissue-specificity of selective estrogen receptor modulators by using a single biochemical method, *Proc. Natl. Acad. Sci. USA*, 2008, **105**, 7171–7176.

[15] F. Fratev, Activation helix orientation of the estrogen receptor is mediated by receptor dimerization: Evidence from molecular dynamics simulations, *Phys. Chem. Chem. Phys.*, 2015, **17**, 13403–13420.

[16] D. J. Kojetin, E. Matta-Camacho, T. S. Hughes, S. Srinivasan, J. C. Nwachukwu, V. Cavett, J. Nowak, M. J. Chalmers, D. P. Marciano, T. M. Kamenecka, A. I. Shulman, M. Rance, P. R. Griffin, J. B. Bruning and K. W. Nettles, Structural mechanism for signal transduction in RXR nuclear receptor heterodimers, *Nat. Commun.*, 2015, **6**, 8013.

[17] M. Okuno, E. Arimoto, Y. Ikenobu, T. Nishihara and M. Imagawa, Dual DNA-binding specificity of peroxisome-proliferator-activated receptor gamma controlled by heterodimer formation with retinoid X receptor alpha, *Biochem. J.*, 2001, **353**, 193-198.

[18] R. Galindo-Murillo, D. R. Roe and T. E. Cheatham III, Convergence and reproducibility in molecular dynamics simulations of the DNA duplex d(GCACGAACGAACGAACGC), *Biochim. Biophys. Acta*, 2015, **1850**, 1041–1058.

[19] C. Bergonzo, N. M. Henriksen, D. R. Roe, J. M. Swails, A. E. Roitberg and T. E. Cheatham III, Multidimensional replica exchange molecular dynamics yields a converged ensemble of an RNA tetranucleotide, *J. Chem. Theory Comput.*, 2014, **10**, 492–499.

[20] Schrödinger Release 2015–2: Maestro, version 10.2, Schrödinger; LLC: New York, NY, USA, 2015.

- [21] D. A. Case, T. A. Darden, T. E. Cheatham III, C. L. Simmerling, J. Wang, R. E. Duke, R. Luo, R. C. Walker, W. Zhang and K. M. Merz, AMBER 14, University of California: San Francisco, CA, USA, 2014.
- [22] J. P. Ryckaert, G. Ciccotti and H. J. C. Berendsen, Numerical integration of the cartesian equations of motion of a system with constraints: molecular dynamics of *n*-alkanes, *J. Comput. Phys.*, 1977, **23**, 327–341.
- [23] H. G. Petersen, Accuracy and efficiency of the particle mesh Ewald method, *J. Chem. Phys.*, 1995, **103**, 3668–3679.
- [24] L. C. T. Pierce, R. Salomon-Ferrer, C. A. F. de Oliveira, J. A. McCammon and R. C. Walker, Routine Access to Millisecond Time Scale Events with Accelerated Molecular Dynamics, *J. Chem. Theory Comput.*, 2012, **8**, 2997-3002.
- [25] P. R. Markwick and J. A. McCammon, Studying functional dynamics in bio-molecules using accelerated molecular dynamics, *Phys. Chem. Chem. Phys.*, 2011, **13**, 20053-20065.
- [26] A. Laio and M. Parrinello, Escaping free-energy minima, *Proc. Natl. Acad. Sci. U.S.A.*, 2002, **99**, 12562–12566.
- [27] A. Barducci, G. Bussi and M. Parrinello, Well-tempered metadynamics: a smoothly converging and tunable free-energy method, *Phys. Rev. Lett.*, 2008, **100**, 020603.
- [28] M. D. Smith, J. S. Rao, E. Segelken and L. Cruz, Force-Field Induced Bias in the Structure of A β 21-30: A Comparison of OPLS, AMBER, CHARMM, and GROMOS Force Fields, *J. Chem. Inf. Model.*, 2015, **55**, 2587-2595.
- [29] F. Fratev, S. Ó. Jónsdóttir and I. Pajeva, Structural insight into the UNC-45-myosin complex, *Proteins*, 2013, **81**, 1212-1221.
- [30] F. Fratev and S. Ó. Jónsdóttir, The phosphorylation specificity of B-RAF (WT), B-RAF (D594V), B-RAF (V600E) and BRAF (K601E) kinases: An in silico study, *J. Mol. Graph. Model.*, 2010, **28**, 598-603.
- [31] E. Harder, W. Damm, J. Maple, C. Wu, M. Reboul, J. Y. Xiang, L. Wang, D. Lupyan, M. K. Dahlgren, J. L. Knight, J. W. Kaus, D. S. Cerutti, G. Krilov, W. L. Jorgensen, R. Abel and R. A. Friesner, OPLS3: A Force Field Providing Broad Coverage of Drug-like Small Molecules and Proteins, *J. Chem. Theory Comput.*, 2016, **1**, 281-296.